

# CHANNEL ESTIMATION PERFORMANCE FOR ZERO-OVERHEAD CHANNEL ACCESS IN MOBILE SENSOR NETWORKS

John E. Kleider, Ghassan Maalouli, Steve Gifford, and Scott Chuprun  
General Dynamics C4 Systems  
Scottsdale, AZ, 85257

Brian Sadler  
U.S. Army Research Laboratory  
Adelphi, MD, 20783

## ABSTRACT\*

*In this work we study the effects of channel estimation/equalization on the BER performance of RF carrier frequency hopped OFDM (FH-OFDM) when using synchronization information that is embedded directly into the OFDM baseband symbol stream. In sensor networks using CSMA, the acquisition preambles can require a large overhead percentage of the overall message. Embedding synchronization information into the data information stream eliminates this channel access overhead, thus providing potential for zero-time overhead channel access. Superposition (embedding) of the sync information, however, causes interference onto the data information, which must be removed for satisfactory BER performance. Consequently, embedded synchronization interference cancellation (EIC) is utilized, which requires accurate channel state estimation. Using coherent 4QAM- and 16QAM-OFDM modulation, channel estimation and BER performance is evaluated using the COST207 multipath fading channel model. Less than a 1 dB performance difference is found between a preamble and embedded system for short message bursts ( $< 1\text{ msec}$ ) and a burst data rate of greater than 1.6 Mbit/sec. The channel estimation mean square error (MSE) versus pilot symbol overhead is also determined as a function of urban and rural channel environments.*

## 1. INTRODUCTION

Orthogonal frequency division multiplexing (OFDM) is being studied extensively for various commercial standards, such as 802.11a, 802.16, asymmetric digital subscriber line (ADSL), and wireless local area networks (WLAN) for spectrally efficient very high data rate wireless services [1]. These standards, however, are not designed to provide operational robustness in mobile fre-

quency hopping (FH) channels used for anti-jam (AJ) operation in Army tactical communications. Wideband Army battlefield communication systems will likely experience harsh time-varying frequency selective fading due to specular changes in the operating environment. Current OFDM standards development activities do not consider high mobility and severe multipath delay spreads. OFDM is, however, an attractive physical layer waveform for ad-hoc networking due to its scalability and spectral efficiency, while providing inherent robustness to multipath fading.

Most of the commercial standards are designed to operate in multipath channels for relatively short transmission range, such that maximum expected multipath delay spread will be small. In this work we adjust the OFDM waveform specifications for longer delay spread environments, with the objective of improving spectral efficiency and channel access efficiency while under RF carrier frequency hopping. Spectral efficiency is improved by directly embedding the synchronization information into the OFDM payload data stream. With this approach, no dedicated time slot is required for a synchronization field. While providing improved bandwidth efficiency, it also provides potential improvement for medium access control. For example, combining an embedded sync field in a TDMA structure could increase the number of available user slots by eliminating the dedicated synchronization field. It also provides improved sensor life in a sensor network, where RF transmission time is a large factor in sensor battery life, and channel access efficiencies using conventional approaches are quite low. Eliminating the dedicated slot for acquisition/synchronization reduces transmission time and thus can lead to a dramatic improvement in battery life for sensor nodes [2].

Superposition (embedding) of the sync information directly into the information symbol stream, causes interference onto the OFDM data information, which must be removed before satisfactory BER performance can be achieved. Consequently, we devise a scheme to perform embedded interference cancellation (EIC), which removes the interference caused by the embedding process onto the data information. However, EIC requires accurate esti-

---

\* Prepared through collaborative participation in the Collaborative Technology Alliance for Communications & Networks sponsored by the U.S. Army Research Laboratory under Cooperative Agreement DAAD19-01-2-0011. The U.S. Government is authorized to reproduce and distribute reprints for Government purposes notwithstanding any copyright notation thereon. The views and conclusions contained in this document are those of the authors and should not be interpreted as representing the official policies, either expressed or implied, of the Army Research Laboratory or the U.S. Government.

Report Documentation Page			Form Approved OMB No. 0704-0188		
Public reporting burden for the collection of information is estimated to average 1 hour per response, including the time for reviewing instructions, searching existing data sources, gathering and maintaining the data needed, and completing and reviewing the collection of information. Send comments regarding this burden estimate or any other aspect of this collection of information, including suggestions for reducing this burden, to Washington Headquarters Services, Directorate for Information Operations and Reports, 1215 Jefferson Davis Highway, Suite 1204, Arlington VA 22202-4302. Respondents should be aware that notwithstanding any other provision of law, no person shall be subject to a penalty for failing to comply with a collection of information if it does not display a currently valid OMB control number.					
1. REPORT DATE <b>00 DEC 2004</b>		2. REPORT TYPE <b>N/A</b>		3. DATES COVERED <b>-</b>	
4. TITLE AND SUBTITLE <b>Channel Estimation Performance For Zero-Overhead Channel Access In Mobile Sensor Networks</b>				5a. CONTRACT NUMBER	
				5b. GRANT NUMBER	
				5c. PROGRAM ELEMENT NUMBER	
6. AUTHOR(S)				5d. PROJECT NUMBER	
				5e. TASK NUMBER	
				5f. WORK UNIT NUMBER	
7. PERFORMING ORGANIZATION NAME(S) AND ADDRESS(ES) <b>John E. Kleider, Ghassan Maalouli, Steve Gifford, and Scott Chuprun General Dynamics C4 Systems Scottsdale, AZ, 85257; U.S. Army Research Laboratory Adelphi, MD, 20783</b>				8. PERFORMING ORGANIZATION REPORT NUMBER	
9. SPONSORING/MONITORING AGENCY NAME(S) AND ADDRESS(ES)				10. SPONSOR/MONITOR'S ACRONYM(S)	
				11. SPONSOR/MONITOR'S REPORT NUMBER(S)	
12. DISTRIBUTION/AVAILABILITY STATEMENT <b>Approved for public release, distribution unlimited</b>					
13. SUPPLEMENTARY NOTES <b>See also ADM001736, Proceedings for the Army Science Conference (24th) Held on 29 November - 2 December 2004 in Orlando, Florida., The original document contains color images.</b>					
14. ABSTRACT					
15. SUBJECT TERMS					
16. SECURITY CLASSIFICATION OF:			17. LIMITATION OF ABSTRACT <b>UU</b>	18. NUMBER OF PAGES <b>8</b>	19a. NAME OF RESPONSIBLE PERSON
a. REPORT <b>unclassified</b>	b. ABSTRACT <b>unclassified</b>	c. THIS PAGE <b>unclassified</b>			

mation of the synchronization offsets and channel perturbations. In a frequency-flat channel, time-frequency offsets and complex scalar channel gain need to be estimated prior to EIC. In a frequency selective fading channel, time-frequency offsets and complex vector channel gain (the channel gain on all OFDM sub-carriers) must be estimated prior to EIC. In this work we assume the channel parameters change from dwell to dwell, requiring fresh channel estimation over each dwell period, while assuming synchronization is perfect. The synchronization algorithms utilized for coarse synchronization [3] and fine synchronization of the time-frequency offsets [4][5] can be used and were found by the authors to produce little degradation in BER performance. Hence in this work, we concentrate on the effects of channel estimation error and its effect on demodulated BER performance.

Pilot signals are used to provide estimates of the channel state. In a frequency-selective fading channel, the number of pilots spread across the frequency-domain OFDM symbol must match the minimum frequency spacing required for satisfactory interpolation of the channel at the OFDM data subcarriers subject to frequency selectivity. Utilizing a known pilot spacing criteria, results show that sufficient BER performance can be achieved using the embedded sync with a FH-OFDM system in a multipath fading channel. We illustrate the available performance of FH-OFDM systems using either 4QAM or 16QAM constellations.

Continuously superimposing (embedding) known information, along with the unknown OFDM data information, can improve channel tracking performance in time-varying channels as shown in [6]. A per-survivor Viterbi receiver is used in [6] to provide the channel estimation and correction but is more complex than conventional OFDM channel estimation techniques, while the performance was found to be highly dependent on the length and choice of PN sequence. In this work we apply embedded sync interference cancellation (EIC) following pilot symbol assisted channel estimation and correction, and use the superimposed sync information for coarse timing, frequency, and phase offset estimation. A description of the coarse synchronization algorithm can be found in [3][7].

Various pilot arrangement techniques for OFDM channel estimation can be found in [8][9] where Least Square (LS) or Minimum Mean-Square (MMSE) estimation and block- or comb-type pilot arrangements are compared. In [8] comb-type pilot arrangement was found to perform better, with less complexity, than the transform domain channel estimator in [10], and in [9] was found to perform better than block-type pilot arrangement. For this work we use comb-type pilot arrangement based on LS channel estimation with optimal pilot spacing as suggested in [11][12]. The comb-type pilot arrangement

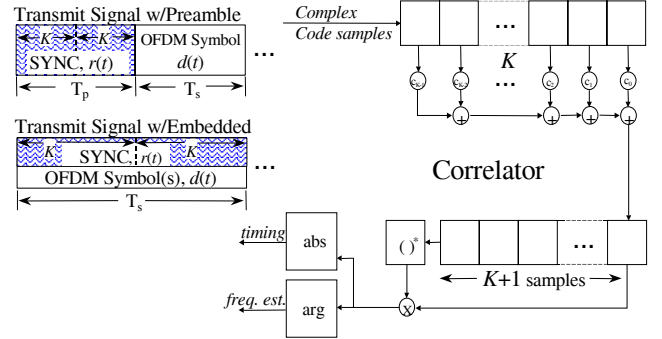


Fig. 1. Preamble- and embedded-based transmit OFDM signal structures (left) and receiver correlator.

transmits known modulation on a subset of the OFDM sub-carrier frequencies in every OFDM symbol and can also be utilized for fine timing, frequency, and phase estimation according to [4][5].

Assuming adequate synchronization is achieved, we utilize LS channel estimation using pilots with spline frequency-domain interpolation [9] along with zero-forcing equalized symbols [13]. We then compare the respective BER performance between the preamble and embedded OFDM systems when transmitted through a fading channel using the COST207 fading model. We also provide expressions for FH rate and bandwidth efficiency between the preamble and embedded synchronization approaches. In Section 2, a description of the OFDM system using embedded coarse synchronization is given. In Section 3, pilot symbol aided channel estimation based on comb-type pilot arrangement and spline interpolation is introduced. In Section 4, FH rate and bandwidth efficiency capability are specified. In Section 5, we provide an analysis of the BER performance of the system. In Section 6, the numerical and simulated results are presented, while Section 7 concludes the paper.

## 2. OFDM TRANSMIT DATA / SYNC STRUCTURES

This section presents a summary of the transmit data structures for each scheme. A more detailed description of the preamble and embedded schemes, with their performance attributes, can be found in [7]. Fig. 1 shows a block diagram of the synchronization scheme for the preamble and embedded signal structures. The same correlator can be used for both methods, and software adjustments can be made to program the correlator length according to the unique performance requirements for each respective scheme. The main parts of the synchronizer (for both methods) are a correlator and a multiplier that multiplies correlator outputs  $K^1$  samples apart. The receiver operating characteristic (ROC) performance of

<sup>1</sup> Note:  $K$  represents the “sub-correlator” length, which is denoted as  $K_p$  and  $K_e$  for the preamble and embedded schemes, respectively.

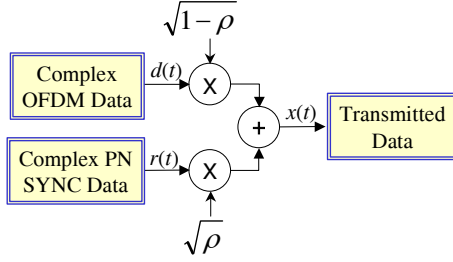


Fig. 2. FH-OFDM embedded sync method.

the correlator is primarily determined by the code length  $K$ , and the received SNR [7]. Time synchronization is achieved by comparing the correlation product to a threshold proportional to the received power. Subsequently, once the detection threshold is crossed, the frequency offset is calculated from the phase of the timing signal.

### 2.1 Embedding Sync With OFDM Payload Data

In a preamble signaling scheme, a time slot is dedicated to the synchronization field immediately prior to the OFDM data symbol(s). For the embedded signaling scheme used in this work, the synchronization information is embedded across all the OFDM payload data samples. When adding the sync information to the OFDM payload, the amplitude of the sync information must be sufficient such that the synchronization works well in low signal to noise ratios. The product of the number of sync code blocks,  $L_e$ , and the length  $K_e$  is set equal to the product of the number of OFDM blocks,  $L_{ofdm}$ , and the time-domain OFDM symbol sample length (including cyclic prefix),  $N_{ofdm}$  per hop dwell period. In the frequency-hopped scenario, the product  $L_{ofdm}N_{ofdm}$  (or  $L_eK_e$ ) should be short to achieve high hop rates. The amplitude ratio of the sync-to-OFDM data payload must be adjusted sufficiently high to satisfy ROC performance requirements at high hop rates.

In this work, the sync information for the embedded approach can be superimposed in the frequency-domain or linearly summed to the time-domain OFDM payload data as shown in Fig. 2. The OFDM data is scaled by  $\sqrt{1-\rho}$  before embedding the synchronization information, which is superimposed at an amplitude level of  $\sqrt{\rho}r[k]$ , where  $r[k]$  is the original synchronization information chip sequence. Both the sync sequence and data sequence have unity power, and when summed together,  $x[k]$  is scaled to ensure that the composite transmitted signal is also near unity power. For a preamble scheme, during the data portion of the transmitted signal,  $x[k] = d[k]$ , and during the sync portion of the signal,  $x[k] = r[k]$ . In the embedded scheme,  $x[k] = \sqrt{1-\rho}d[k] + \sqrt{\rho}r[k]$ .

### 3. PILOT SYMBOL AIDED CHANNEL ESTIMATION

For this work we use comb-type pilot arrangement based on LS channel estimation with optimal pilot spacing as suggested in [11][12]. The comb-type pilot arrangement transmits known modulation on a subset of the OFDM sub-carrier frequencies in every OFDM symbol and can also be utilized for fine timing, frequency, and phase estimation according to [4][5]. The comb-type arrangement we use is a form of the periodic arrangement described in [11]. In a FH system, we assume that a sufficient hop rate can be attained such that the channel is approximately constant over each dwell period. This implies that the symbol portion of the dwell time is less than or equal to the channel coherence time, such that the complex vector channel gain across all OFDM sub-carriers stays fixed for each dwell period. We also assume that the channel changes for each hop frequency, such that fresh channel estimation is required for each dwell period, and that these parameters are uncorrelated from hop to hop.

In the following, we denote all OFDM sub-carriers as  $X$ .  $X(i_p)$  is a vector of pilot symbols, where  $i_p$  denotes the pilot sub-carrier frequency locations, and for simplicity we denote  $X(i_p)$  as  $X^p$  such that  $X^p \in X$ . The data and null sub-carrier symbols are denoted as  $X(i_d)$  and  $X(i_n)$ , respectively, where  $i_d$  and  $i_n$  denote the data and null sub-carrier frequency locations, respectively. Again, for notational simplicity, we denote  $X(i_d)$  and  $X(i_n)$  as  $X^d$  and  $X^n$ , where  $X^d, X^n \in X$ . Further, we denote  $X^{dp}$  as the variable containing both the pilot and data information, such that  $X^p, X^d \in X^{dp} \in X$ , where  $i_{dp}$  contains all pilot and data sub-carrier locations. In the comb-type arrangement [12], the pilot frequency spacing is,

$$N_F = 1/(2f_{sub}\tau_{max}), \quad (1)$$

and the pilot time spacing is

$$N_T = 1/(2f_{Dmax}T_s), \quad (2)$$

respectively, where  $\tau_{max}$  is the maximum expected delay spread and  $f_{Dmax}$  is the maximum expected Doppler spread.

In a comb-type arrangement, the transmitted pilot sequence,  $X^p$ , is generated by placing  $N_p$  pilots uniformly across  $X^{dp}$  as suggested in [9][11]. We define  $H^p$  as the complex channel gain at the pilot sub-carriers. The LS estimate of the channel at the pilot sub-carriers is then

$$\hat{H}^p = Y^p/X^p, \quad (3)$$

where  $Y^p$  is the received pilot sequence through the channel at sub-carrier locations specified by  $i_p$ . We note that LS channel estimation is susceptible to noise and ICI, but

we utilize LS estimation to minimize complexity. Better channel estimation methods are available, such as MMSE [9], but are more complex. Following LS estimation at the pilot frequencies, the channel estimates at the data sub-carriers are found using *spline interpolation*. The spline interpolation technique was found to provide good results when comparing various interpolation techniques [9].

#### 4. FREQUENCY HOPPING RATE AND BANDWIDTH EFFICIENCY

We use the same frequency hopping structure as specified in [7]. Both OFDM schemes utilized 75% of  $N$  (total number of OFDM sub-carriers) for the number of data bearing plus pilot sub-carriers, represented as  $X^{dp}$  in Section 3. The unused sub-carriers,  $X^n$ , are set to null carriers. For the preamble and embedded schemes, according to the comb-type arrangement, the pilot overhead will be determined by  $N_T$  and  $N_F$ . For this work  $N_T = 1$ , while the value of  $N_F$  depends on the maximum expected delay spread,  $\tau_{\max}$ , according to (1).

In a preamble scheme the hop duration is [7]

$$T_h = T_p + L_{ofdm}(T_s + T_g) + T_{sw}, \quad (4)$$

where  $T_p$  is the preamble time,  $T_s$  is the OFDM symbol time,  $T_g$  is the guard interval time, and  $T_{sw}$  is the switch duration (dead time plus rise and fall times) between hop frequencies [14]. For the embedded scheme the hop duration is [7]

$$T_h = L_{ofdm}(T_s + T_g) + T_{sw} - T_g. \quad (5)$$

In the embedded scheme, the first guard interval is not required if we assume that the switch interval can act as a guard time between hop frequencies. In the preamble scheme, the first guard interval is required to prevent ISI between the preamble and the first OFDM symbol for that hop frequency.

We define bandwidth efficiency as the transmitted bit rate divided by the RF bandwidth per hop frequency or

$$\eta = \frac{\log_2 M (N - N_n - N_p) L_{ofdm} R_h}{B} \text{ (bits/s/Hz)}, \quad (6)$$

where  $M$  is the  $M$ -QAM modulation order,  $N$  is the total number of OFDM sub-carriers,  $N_n$  is the number of null sub-carriers,  $N_p$  is the number of pilots,  $L_{ofdm}$  is the number of OFDM symbols per dwell,  $R_h = 1/T_h$  is the hop rate in hops/s, and  $B = (N - N_n - N_p)f_s/N$  is the RF bandwidth per hop, and  $f_s$  is the base-band sampling rate. Achievable bandwidth efficiency, as a function of hop rate, can be determined for equivalent ROC performance by using equations (4) – (6) and (13) from [7].

#### 5. BER ANALYSIS IN FREQUENCY SELECTIVE FADING

In this section we derive an approximate analytical expression for BER of  $M$ -QAM OFDM modulation under frequency selective fading with channel estimation error for both the preamble and embedded systems. In this work the frequency selective channel distortion is compensated with zero-forcing equalization using channel estimates as described in Section 3. Analysis in [13] provides a closed form approximation of the BER performance in time-varying frequency-selective fading channels. We modify the results in [13] for the embedded synchronization scheme. While our focus is to predict performance for the embedded scheme, the expressions we develop can also be applied to the preamble scheme by setting  $\rho = 0$ .

##### 5.1 Signal Model

When the transmitted OFDM signal is affected by a frequency offset  $\varepsilon$ , the received OFDM symbol from the  $N$ -point IFFT modulator [15] is given by

$$y[k] = \frac{1}{\sqrt{N}} \sum_{m \in X^{dp}} H[m] X[m] e^{j2\pi k(m+\varepsilon)/N} + w[k], \quad (7)$$

where  $X[m]$  and  $H[m]$  are the data symbol and channel response of the  $m^{\text{th}}$  sub-carrier,  $w[k]$  is the additive receiver noise, and  $X^{dp}$  is as defined in Section 3. With ideal timing, the output of the FFT demodulator for the  $l^{\text{th}}$  sub-carrier is

$$\begin{aligned} Z[l] &= \frac{1}{N} \sum_{k=0}^{N-1} \sum_{m \in X^{dp}} H[m] X[m] e^{j2\pi k(m+\varepsilon)/N} e^{-j2\pi kl/N} + W[l] \\ &\equiv Z_l = H_l^\varepsilon X_l + I_l + W_l \\ &= H_l^\varepsilon (\sqrt{1-\rho} D_l + \rho R_l) + I_l + W_l, \end{aligned} \quad (8)$$

where  $X_l = \sqrt{1-\rho} D_l + \sqrt{\rho} R_l$ ,  $W_l$  is the frequency-domain additive noise,  $I_l$  and  $H_l^\varepsilon$  are the inter-carrier interference (ICI) and distorted channel response, respectively, due to frequency offset and fading as found in [13].  $D_l$  and  $R_l$  are the frequency-domain versions of variables  $d$  and  $r$ , respectively, as shown in Section 2.1. The estimated channel response can be written as  $\hat{H}_l^\varepsilon = H_l^\varepsilon + v_l$ , where  $v_l$  denotes the channel estimation error of the  $l^{\text{th}}$  sub-carrier. Combining (8) and the estimated channel response, the zero-forcing equalized symbol is found to be

$$\begin{aligned} \hat{D}_l &= \frac{\hat{H}_l^\varepsilon Z_l}{|\hat{H}_l^\varepsilon|^2} = \\ &\left(1 - \frac{v_l}{\hat{H}_l^\varepsilon}\right) \sqrt{1-\rho} D_l + \left(1 - \frac{v_l}{\hat{H}_l^\varepsilon}\right) \sqrt{\rho} R_l + \frac{I_l + W_l}{\hat{H}_l^\varepsilon}. \end{aligned} \quad (9)$$

Following embedded interference cancellation (EIC) ( $-\sqrt{\rho}R_l$ ) and scaling of the leftover data by  $1/\sqrt{1-\rho}$ , the estimated data symbol can be written as

$$\hat{D}_l = \left(1 - \frac{v_l}{\hat{H}_l^\varepsilon}\right) D_l - \left(\frac{v_l}{\hat{H}_l^\varepsilon}\right) \frac{\sqrt{\rho}}{\sqrt{1-\rho}} R_l + \frac{I_l + W_l}{\sqrt{1-\rho} \hat{H}_l^\varepsilon}. \quad (10)$$

## 5.2 Fading Channel Performance

Assuming the channel response is stationary over more than one symbol, the effective SNR of the  $l$ th sub-carrier can be written as

$$\gamma_\varepsilon^l = \frac{|H_l^\varepsilon + v_l|^2}{\left(1 + \frac{\rho}{1-\rho}\right) |v_l|^2 + \sigma_e^2}, \quad (11)$$

where  $\sigma_e^2$  is the normalized interference signal power,  $(\sigma_I^2 + \sigma_W^2)/(1-\rho)\sigma_X^2$ , and  $\sigma_I^2$ ,  $\sigma_W^2$ ,  $\sigma_X^2$  are the ICI, noise, and received signal powers, respectively.

Assuming the channel is normalized, such that  $E[|H|^2] = 1$ , the average effective SNR is found to be [13]

$$\gamma_\varepsilon = [(\sin(\pi\varepsilon)/\pi\varepsilon)^2 - \sigma_e^2] I(a, b) + 1, \quad (12)$$

where  $I(a, b) = \frac{e^{a/b}}{b} \text{Ei}(a/b)$ , Ei is the expectation integral,  $a = \sigma_e^2$ , and  $b = \sigma_v^2$ , representing the channel estimation error variance. Assuming the Rayleigh channel is normalized and stationary over each hop duration, the average BER of  $M$ -QAM can be approximated as

$$P_B \cong \frac{2(\sqrt{M}-1)}{\sqrt{M} \log_2 M} \left(1 - \sqrt{\frac{c(1+\sigma_v^2)\gamma}{c(1+\sigma_v^2)\gamma + 2(M-1)(1+\sigma_v^2\gamma)}}\right) \quad (13)$$

where  $\gamma$  is the average received signal-to-noise ratio and  $c \cong 9.5$ . (12) and (13) provide an approximate analytical solution for calculating the BER when using either the embedded ( $0 < \rho < 1$ ) or preamble ( $\rho = 0$ ) schemes.

## 6. NUMERICAL AND SIMULATED RESULTS

This section presents numerical results for a FH-OFDM system where,  $N_T = 1$ ,  $N_F = 10$ ,  $L_{ofdm} = 4$  and  $L_e = 10$ . We assign  $K_p = 16$  and  $K_e = 128$ , where in (4)  $T_p = 2K_p T$ ,  $f_s = 1.333 \times 10^6$ ,  $N = 256$ , with  $N_p = 20$  pilot sub-carriers and  $T_{sw} = T_g = 15 \mu s$ . Later we also present the channel estimator MSE performance as a function of pilot overhead and channel type. The OFDM modulator specs are the same for the preamble and embedded schemes.

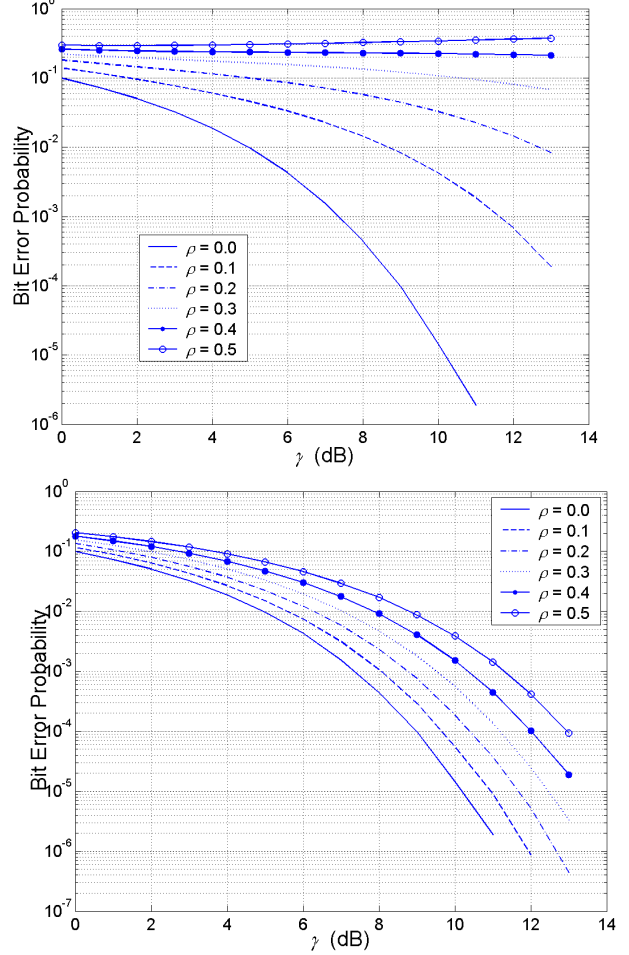


Fig. 3. FH-OFDM 4QAM BER performance without EIC (top) and with EIC (bottom).

Given these design parameters, the hop rates and bandwidth efficiencies are 1153 and 1208 hops/s, and 1.59 and 1.66 bits/s/Hz, respectively for the preamble and embedded schemes. The channel is assumed to be constant over each hop dwell but uncorrelated between consecutive dwell intervals. Simulated BER performance results are presented for both FH-OFDM schemes using 200k (68.8 Mbits) and 20k (6.88 Mbits) OFDM simulated data symbols in the AWGN and fading channels, respectively. Analytical performance estimates using (13) were found to corroborate the simulated BER performance results using the TU fading channel model.

### 6.1 AWGN Channel EIC Performance

In this section we provide simulated BER performance in AWGN with synchronization offsets. We induce a random timing offset, a frequency offset of 300 Hz and a carrier phase offset of 40 degrees. Fig. 3 shows the BER results when EIC is (bottom) and is not (top) utilized, respectively. When EIC is utilized, the only performance loss is due primarily to the SNR degradation from the  $\sqrt{1-\rho}$  data signal loss factor induced at the

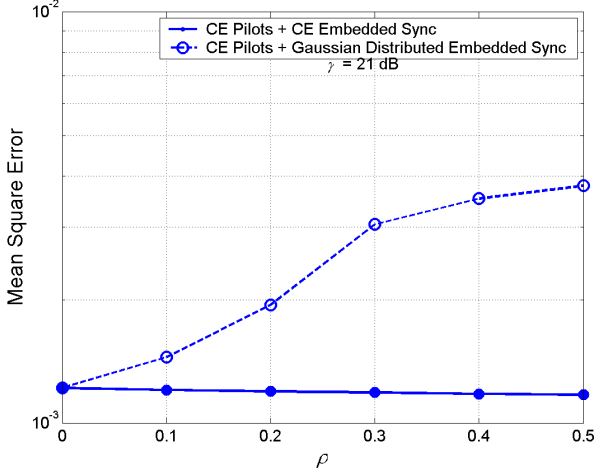


Fig. 4. MSE of LS channel estimator with spline interpolation as a function of  $\rho$  for  $\gamma = 21$  dB.

transmitter, with an imperceptible loss due to a small residual sync estimation error. It is clear that the EIC is critical, even for the benign AWGN channel.

## 6.2 Fading Channel Estimation Error

In this work, the pilot spacing in time is  $N_T = 1$  and using (1), the pilot spacing in frequency, assuming  $\tau_{\max} = 10 \mu\text{s}$ , is  $N_F \cong 10$ , assuming the modulator design parameters described above. From Section 5, it is evident that the BER will be dependent on the level at which the embedded sync is superimposed at the transmitter.  $\sigma_e^2$  and  $\sigma_v^2$  will be the primary factors affecting the embedded scheme demodulated BER. With high SNR and low frequency offset,  $\sigma_v^2$  will dominate because it will detrimentally affect our ability to perform EIC (due to noisy channel estimation).

The question we answer in the following is whether or not  $\rho$  affects the channel estimation error as a function of  $\gamma$ . To address this issue, it is important to note that channel estimation quality is determined primarily by the pilot signal, which is generated in the frequency domain. In [16] optimal training sequences are studied based on their MSE performance. Typically the sub-carrier pilot signal is a constant envelope (CE) signal that is orthogonal to the data sub-carriers, and as long as we maintain this property, even after embedded sync superposition, then the error variance of the channel estimate will be unchanged when  $\rho > 0$ , and the embedded sync signal values across the data sub-carriers can be chosen as desired. From this we deduce the following constraint:

*Constraint 1 - The embedded sync signal, at the pilot sub-carrier locations in the frequency domain, must be as-*

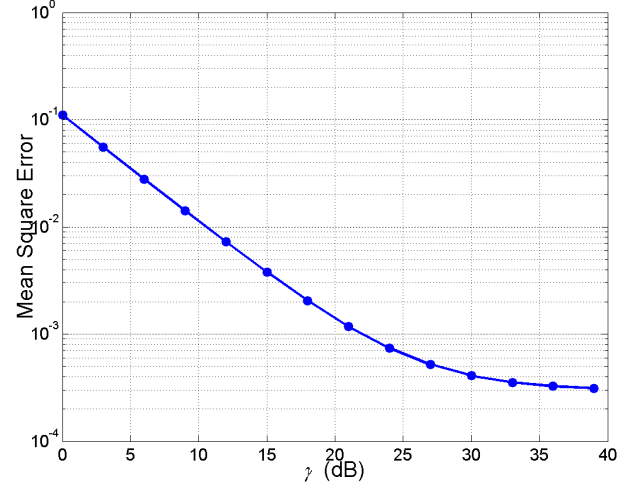


Fig. 5. MSE of LS channel estimator as a function of  $\gamma$  for TU channel.

*signed the same values as the pilot signal. Given that the pilot modulation is constant amplitude, this ensures constant amplitude after embedded sync is superimposed onto the pilot modulation.*

*Constraint 1* simply ensures that the estimation variance is due only to the receiver noise, frequency-selective channel gain, and quality of the channel estimator, and not due to additional variance caused by a non-constant envelope signal added to the pilot signal.

Fig. 4 illustrates the MSE of the channel estimator, over 1000 channel realizations at  $\gamma = 21$  dB, either when the embedded sync signal does or does not comply with *Constraint 1* as a function of  $\rho$ . We see that, for the non-CE (Gaussian distributed) case, the MSE increases with increasing embedding factor  $\rho$ . Under *Constraint 1*, Fig. 5 illustrates the overall MSE as a function of SNR. Ideally, the MSE should decrease linearly with increasing SNR [16]. However, in our case a MSE floor is apparent at approximately  $3 \times 10^{-4}$ . We believe this MSE floor is due primarily to the inability of the spline interpolator to adequately track the data sub-carrier frequency selectivity between the pilot sub-carrier locations, causing irreducible estimation error at high  $\gamma$ . This suggests that  $N_F < 10$  may be appropriate for the TU channel.

## 6.3 Perfect Channel Estimation

Simulated BER performance results are presented for both preamble ( $\rho = 0$ ) and embedded ( $0.1 \leq \rho \leq 0.5$ ) FH-OFDM systems with 4QAM (see Fig. 6) and 16QAM (see Fig. 7), with perfect channel estimation. For the embedded cases of both figures, the only apparent penalty is due to loss of signal power ( $\sqrt{1-\rho}$  factor). At  $\rho = 0.5$ , a  $\gamma$  loss of 3 dB is apparent.

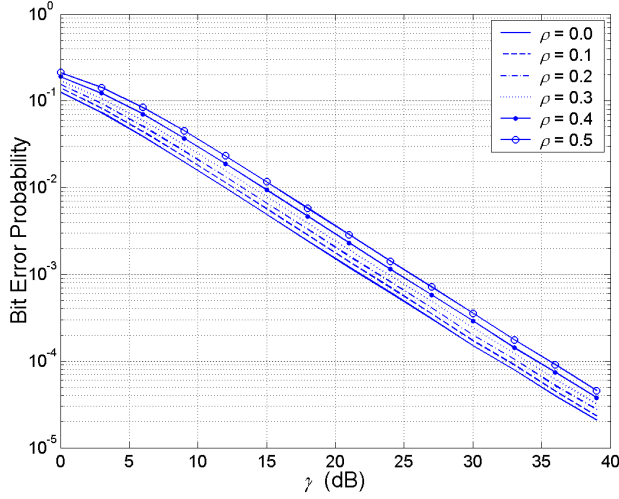


Fig. 6. 4QAM BER, perfect channel estimation.

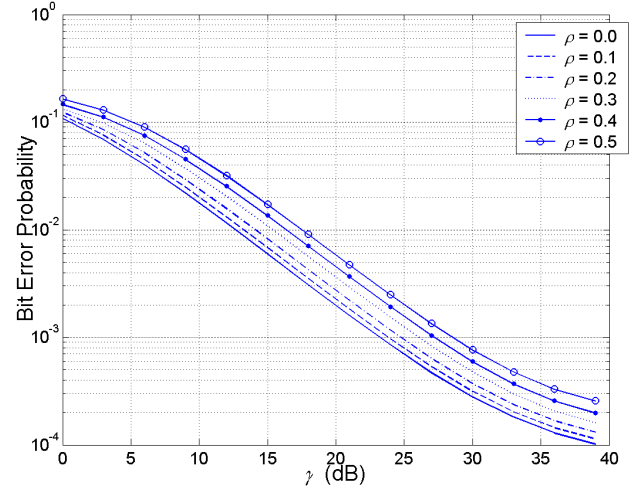


Fig. 8. 4QAM BER, actual channel estimation.

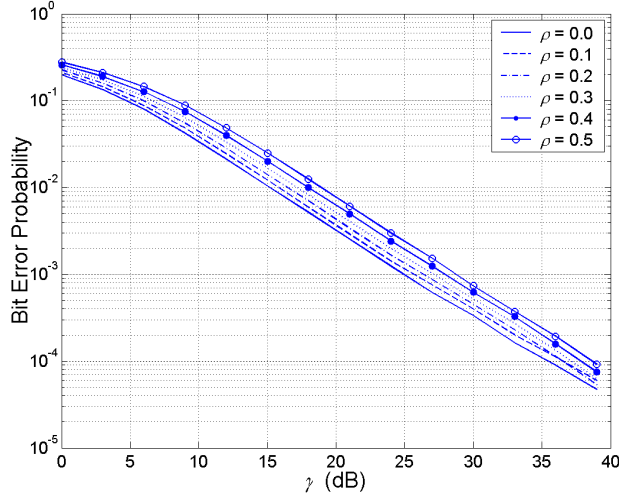


Fig. 7. 16QAM BER, perfect channel estimation.

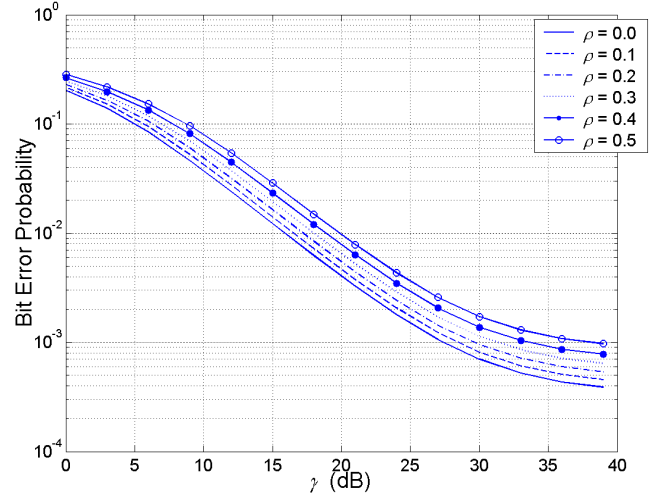


Fig. 9. 16QAM BER, actual channel estimation.

#### 6.4 Non-Perfect Channel Estimation

Simulated BER performance results are presented for 4QAM (see Fig. 8) and 16QAM (see Fig. 9), using actual channel estimates. For the embedded cases, the BER penalty is due to loss of signal power ( $\sqrt{1-\rho}$  factor) and due to non-perfect EIC resulting from imperfect channel estimation. Eq. (13) was found to provide a good approximation of the performance shown in Figs. 6 – 9. At low  $\gamma$ , (13) is less accurate. For perfect channel estimation,  $\sigma_e^2$  dominates due to the noise variance part  $\sigma_W^2$ . For actual channel estimation,  $\sigma_e^2$  dominates due to the noise variance part  $\sigma_W^2$  at lower to mid-range  $\gamma$  but at high  $\gamma$ ,  $\sigma_v^2$  dominates causing a BER floor, which is a direct effect of the MSE floor seen in Fig. 5.

#### 6.5 Pilot Overhead and Channel Type

The previous results show that our channel estimation method is sufficiently accurate to produce low demodulated BER in mobile frequency-selective channels. Also, we showed the importance of following *Constraint 1* for minimum channel estimator MSE (ref. Fig. 4). Fig. 10 shows the estimator MSE performance versus pilot symbol assisted channel estimation overhead and channel type with an embedding factor,  $\rho = 0.1$  and a average received signal-to-noise ratio,  $\gamma = 21$  dB. From the results we see that the estimator reaches its minimum MSE for the RA and TU channels at approximately 4% and 14%, respectively.

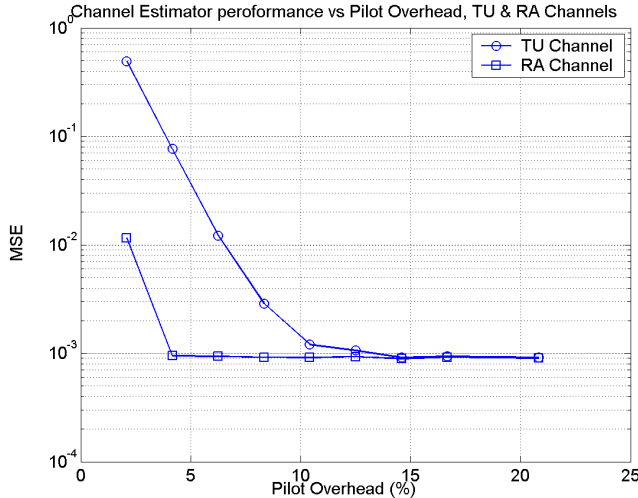


Fig. 10. Channel estimator MSE as a function of pilot overhead and channel type for  $\gamma = 21$  dB snr.

## CONCLUSION<sup>#</sup>

This paper showed that OFDM BER performance degrades less than 1 dB when using embedded synchronization ( $\rho = 0.1$ ) compared to preamble synchronization ( $\rho = 0$ ) in multipath fading with embedded interference cancellation. Low complexity channel estimation provides sufficiently low mean square error to provide good demodulation performance for both 4QAM and 16QAM modulations with FH-OFDM. From our results, hop dwell times of less than 1 msec can be supported with this system. Alternatively, we could consider this system applicable to highly mobile environments where the channel coherence time is greater than 1 msec. We believe that this system could support higher hop rates by using more accurate channel estimation and spatial diversity.

## REFERENCES

- [1] S. Ariyavisitakul, D. Falconer, F. Adachi, and H. Sari, "Guest editorial – wireless broadband techniques," *IEEE JSAC*, vol. 17, no. 10, pp. 1709-1710, Oct., 1999.
- [2] [http://www.darpa.mil/ato/solicit/CN/cn\\_brief.pdf](http://www.darpa.mil/ato/solicit/CN/cn_brief.pdf)
- [3] J. Kleider and S. Gifford, "Synchronization for broadband OFDM mobile ad hoc networking: simulation and implementation," in *Proc. of ICASSP*, vol. 4, pp. 3756-3759, 2002.
- [4] D. Kim, S. Do, H. Cho, H. Choi, and K. Kim, "A new joint algorithm of symbol clock adjustment for OFDM systems," *IEEE Trans. on Cons. Electron.*, vol. 44, no. 3, pp. 1142-1148, Aug. 1998.

- [5] D. Matic, N. Petrochilos, A. Trindade, F. Schoute, P. Common, and R. Prasad, "OFDM synchronization based on the phase rotation of sub-carriers," in *Proc. of VTC*, vol. 2, pp. 1260-1264, May, 2000.
- [6] P. Hoeher and F. Tufvesson, "Channel estimation with superimposed pilot sequence," in *Proc. of Globecom*, pp. 2162-2166, Dec. 1999.
- [7] J. Kleider, S. Gifford, G. Maalouli, S. Chuprun, and B. Sadler, "Synchronization for RF carrier frequency hopped OFDM: analysis and simulation," in *Proc. of MILCOM*, Oct. 2003.
- [8] M. Hsieh and C. Wei, "Channel estimation for OFDM systems based on comb-type pilot arrangement in frequency selective channels," *IEEE Trans. Consumer Electron.*, vol. 44, no. 1, pp. 217-225, Feb. 1998.
- [9] S. Coleri, M. Ergen, A. Puri, and A. Bahai, "Channel estimation based on pilot arrangement in OFDM systems," *IEEE Trans. Broadcasting*, vol. 48, no. 3, pp. 740-741, Sep. 2002.
- [10] Y. Zhao and A. Huang, "A novel channel estimation method for OFDM mobile communications systems based on pilot signals and transform domain processing," in *Proc. of VTC*, pp. 2089-2093, May 1997.
- [11] M. Dong, L. Tong, and B. Sadler, "Optimal pilot placement for channel tracking in OFDM," in *Proc. of MILCOM*, vol. 1, pp. 602-606, Oct. 2002.
- [12] F. Tufvesson and T. Maseng, "Optimization of sub-channel bandwidth for mobile OFDM systems," in D. Everitt and M. Rumsewicz, editors, *Multi-access, mobility and teletraffic – advances in wireless networks*, pp. 103-114, Kluwer Academic Publishers, Dordrecht, The Netherlands, 1998.
- [13] H. Cheon and D. Hong, "Effect of imperfect channel information in OFDM-based WLAN," *IEEE Electron. Let.*, vol. 38, no. 16, pp. 912-914, Aug., 2002.
- [14] D.J. Torrieri, *Principles of Secure Communication Systems*, 2<sup>nd</sup> Ed., Artech House, 1992.
- [15] P.H. Moose, "A technique for orthogonal frequency division multiplexing frequency offset correction," *IEEE Trans. Commun.*, vol. 42, no. 10, pp. 2908-2914, Oct., 1994.
- [16] T.-L. Tung and K. Yao, "Channel estimation and optimal power allocation for a multiple-antenna OFDM system," *EURASIP JSAP*, 3, pp. 1-10, 2002.

<sup>#</sup> The views and conclusions contained in this document are those of the authors and should not be interpreted as representing the official policies, either expressed or implied, of the Army Research Laboratory or the U.S. Government.